



## New Mo–V based oxidic precursor for the hydrotreatment of residues

Deana Soogund<sup>a</sup>, Philippe Lecour<sup>a</sup>, Antoine Daudin<sup>a,\*</sup>, Bertrand Guichard<sup>a</sup>,  
Christelle Legens<sup>a</sup>, Carole Lamonier<sup>b</sup>, Edmond Payen<sup>b</sup>

<sup>a</sup> IFP-Lyon, BP N° 3, 69360 Solaize, France

<sup>b</sup> Université de Lille1, Unité de Catalyse et de Chimie du Solide, Bâtiment C3, 59650 Villeneuve d'Ascq, France

### ARTICLE INFO

#### Article history:

Received 24 November 2009

Received in revised form 20 April 2010

Accepted 26 April 2010

#### Keywords:

Catalysis  
Hydrodemetallation  
Heteropolyanions  
Vanadium  
Molybdenum  
Sulphide

### ABSTRACT

In order to understand the role of vanadium and its interaction with molybdenum atoms in the catalysts used for the hydrotreatment of residues, mixed heteropolyanion (HPA) precursors  $\text{PMo}_{(12-x)}\text{V}_x\text{O}_{40}^{(3+x)-}$  have been prepared and deposited by incipient wetness impregnation on an alumina support. The evolution of the compounds in the impregnating solutions till their deposition on the support has been analysed using various spectroscopic techniques such as Raman,  $^{31}\text{P}$  and  $^{51}\text{V}$  NMR, XPS as well as TEM. Activity measurements on model molecules (toluene and cyclohexane) and on real feedstock (vacuum residue) have been performed after activation step (*ex situ* sulphidation). Hydrogenation (HYD), isomerisation (ISOM), hydrodemetallation (HDM), hydrodesulphurisation (HDS), hydrodeasphaltenisation (HDAsC<sub>7</sub>) were assessed. During tests (2 h) on a Safaniya vacuum residue feed, interesting HDM activity was observed compared to reference promoted and unpromoted catalysts (NiMo and Mo/Al<sub>2</sub>O<sub>3</sub>). It can be concluded that the use of vanadium in the impregnating solution may promote HDM and HDAsC<sub>7</sub> (increase of vanadium removal rate around 15% compared to Mo-catalyst without vanadium). Furthermore HDM and HDAsC<sub>7</sub> catalytic performances turned out to be close to the ones of NiMo catalyst. The increase in HDM/HDAsC<sub>7</sub> activity may be related to the improvement of hydrogenation and/or isomerisation, the latter being improved by the presence of vanadium.

© 2010 Elsevier B.V. All rights reserved.

### 1. Introduction

In the petroleum industry, it is well known that it is desirable to treat heavy hydrocarbon feedstock and particularly petroleum residue so as to obtain lighter hydrocarbon feedstock characterised by a higher economic value. Petroleum residue consists of four component classes as follows: saturated, aromatics, resins and asphaltenes. Very large molecules such as vanadium or nickel porphyrins are mainly contained in asphaltenes and can be either of continental type [1], i.e. when there is a pericondensed polyaromatic layer comprising heterocycles (N, S), supporting functional groups (oxygenated in particular) and alkyl substituents, or of archipelago type [2], i.e. when aromatic nuclei are linked with alkyl heteroatomic or non-heteroatomic chains.

Large quantities of catalysts are used in the industry for the purification and the upgrading of various petroleum streams and residues. These processes known as hydrotreatment [3] are involved in the removal of heteroatoms such as sulphur (hydrodesulphurisation), nitrogen (hydrodenitrogenation) and

metals such as nickel and vanadium (hydrodemetallation). This study focuses on the upgrading of petroleum residue through the demetallation process. Metals must be removed from crude oil since they poison catalysts during the hydrodesulphurisation and cracking of the feeds.

Hydrodemetallation (HDM) is usually carried out in a trickle-bed reactor or ebullated-bed reactor at high temperature and pressure with hydrotreating catalysts with supports having a specified range of pores. The mesopores with pore having relatively small diameters (diameter  $\approx$  10–50 nm) in which the active phase develops and the macropores with pores having relatively large diameters (diameter  $>$  50 nm) which facilitate the diffusion of asphaltenes and resins to the active phase [4,5]. The active phase generally consists of MoS<sub>2</sub> nanocrystallites well dispersed on a high specific surface area alumina support with cobalt or nickel as promoter [6–8]. The active phases are obtained through the sulphidation of an oxidic precursor prepared by incipient wetness impregnation of a  $\gamma$  or  $\delta$  alumina support with aqueous solution containing the elements to be deposited.

A significant proportion of metals present in heavy oil is typically in the form of porphyrins which decompose on the surface of catalysts during refining processes, thus leading to a decrease in catalytic performances. For example, the maximum metal content on the spent catalyst with an atmospheric residue from Kuwait

\* Corresponding author at: IFP-Lyon, Direction Catalyse et Séparation, Rond Point de l'échangeur de Solaize, 69360 Solaize, France. Tel.: +33 0 478022020.

E-mail address: [antoine.daudin@ifp.fr](mailto:antoine.daudin@ifp.fr) (A. Daudin).

Export Crude after 9720 h of a life test is approximately 24.5% (w/w) of metal (V + Ni)/100 g of fresh HDM catalyst [9].

In the literature there have been various studies on how metal porphyrins attach to the catalyst surfaces [10–12] during hydrometallation (HDM). The role of the deposited vanadium on the catalytic performances is of paramount importance since the catalyst can take up large amounts of vanadium [9]. Vanadium sulphide derivatives were suspected to form on the catalyst surface after the degradation step of the petroporphyrins. Nevertheless the authors did not agree on their exact nature and the proposed stoichiometry of vanadium sulphide phases were mainly  $V_2S_3$  [13–15],  $V_3S_4$  [16,17] and  $V_5S_8$  [18,19].

The catalytic properties of vanadium sulphides have hardly been studied. In the early 1980s, Sie [20] proposed that metal deposits could act as HDM catalysts. Toulhoat et al. [21] studied the activity of a macroporous alumina under feed. It was shown that activity increased with time of stream and an interesting HDM conversion was observed as well as a high performance in the conversion of asphaltenes. This activity was ascribed to Ni and V deposits on the alumina surface. Hubaut et al. [22,23] examined the activity of spent catalysts in toluene hydrogenation (HYD). The  $MoS_2$  catalyst showed an increase in HYD activity with the progressive vanadium deposit whereas the Ni– $MoS_2$  catalyst showed the inverse trend. Ledoux et al. [24] considered the activity of a  $V_xS_y/Al_2O_3$  catalyst in thiophene HDS. The activity was 30 times lower than the activity of a NiMo catalyst. It appears that the properties of vanadium sulphide catalysts remain a point of controversy in the literature and these discrepancies may be ascribed to the complexity of the vanadium sulphide system and the impact of vanadium on the  $MoS_2$  activity.

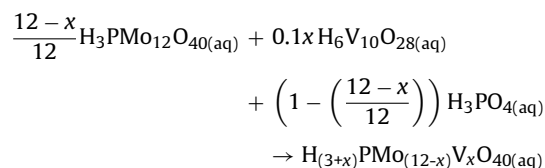
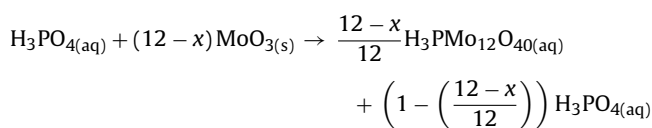
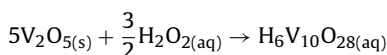
The aim of this paper is to understand the role of vanadium and its interaction with Mo atoms when both metals are introduced in the same structure. For that, mixed heteropolyanion (HPA) precursors  $PMo_{(12-x)}V_xO_{40}^{(3+x)-}$  generally used in the field of oxidation catalysis have been prepared and deposited on alumina support by incipient wetness impregnation [25,26]. After the description of the preparation of the oxidic precursors, the nature of the deposited species will be discussed as well as their evolution at each step of the preparation through a detailed characterisation with various typical techniques. Finally these new precursors were sulphided and the morphology of the active phase was studied. Furthermore, their catalytic performances were evaluated on model molecules as well as on vacuum residue and were compared to those obtained with more conventional hydrotreating catalysts:  $MoS_2$  and Ni– $MoS_2$  supported catalysts. All these results will allow us to discuss the origin of the beneficial effect of the use of vanadium combined with molybdenum as a HDT catalyst.

## 2. Experimental

### 2.1. Preparation

#### 2.1.1. Preparation of the heteropolyanions (HPA)

The Keggin phosphomolybdate HPAs,  $H_{(3+x)}PMo_{(12-x)}V_xO_{40}$  with  $x = 1, 3$  and  $6$ , were prepared according to the Odyakov et al. [26] method. The starting materials were the well-known pure heteropolyacid  $H_3PMo_{12}O_{40}$  and an aqueous solution of decavanadic acid ( $H_6V_{10}O_{28}$ ) obtained by dissolving  $V_2O_5$  in a cold 30%  $H_2O_2$  solution. The decavanadic acid was then gradually added under stirring to the heteropolyacid maintained at 363 K. The amount of solid added was done according to the vanadium to molybdenum atomic ratio in the awaited HPA. The following equations describe the reaction steps for the formation of the heteropolyanions:



The HPA is obtained directly in an aqueous solution which can be used for the preparation of the oxidic precursor. Table 1 presents the various solutions that have been prepared with the V/Mo atomic ratios which will be used hereafter. In this table, the Mo/P and V/ $H_2O_2$  molar ratios used for the preparations of the starting solutions are also reported. During the synthesis we encountered difficulties with the Odyakov's method for the preparation of the highest V/Mo ratio equal to 1 due to a lack of solubility of  $V_2O_5$  [26]. This solution was thus obtained by dissolution of  $MoO_3$  in  $H_2O_2$  with a Mo/ $H_2O_2$  molar ratio of 1/6. After complete dissolution, phosphoric acid was added followed by a gradual addition of  $V_2O_5$ . The Mo/P ratio was the same.

Aqueous solutions have been prepared in order to obtain a 9 wt.%  $MoO_3$  catalyst which implied the use of 0.54, 1.91 and 5.74 wt. % of  $V_2O_5$  for molar ratios of V/Mo = 1/11, 3/9 and 1 respectively. The three solutions will be designated as A«Sol», B«Sol» and C«Sol» according to their V/Mo ratios (A: V/Mo = 1/11, B: V/Mo = 3/9 and C: V/Mo = 1).

#### 2.1.2. Preparation of the catalyst

The oxidic precursors were obtained by incipient wetness impregnation of the aforementioned aqueous solutions (A«Sol», B«Sol» and C«Sol») on beads of alumina. This support comprised two types of pores: mesopores and macropores.

After overnight maturation, in order to let the species diffuse into the alumina beads, the solids were dried under air at 393 K and then calcined at 773 K for 2 h under air. The impregnated solid after the drying and calcination steps has been described as oxidic precursor hereafter. The composition of the catalyst (wt% molybdenum oxide and vanadium oxide) present in the oxidic precursors is reported in Table 1.

The oxidic precursors were sulphided at 623 K under atmospheric pressure with a  $H_2/H_2S$  (15% mol.) mixture and a gas flow of 2 L/h/g of catalyst. The sulphided catalysts used for characterisation purposes were transferred into glass vials under vacuum in order to avoid any contact with air.

For comparison purposes a reference catalyst without vanadium but having the same molybdenum loading and a P/Mo ratio corresponding to 1/11 has been prepared by impregnation with a solution obtained by dissolving  $MoO_3$  in a phosphoric acid solution. [27]. It is designated as RefMoP. After incipient wetness impregnation and maturation, this classical solid was then dried and calcined under the same conditions as those used for the HPA-based oxidic precursors. A classical NiMoP/ $Al_2O_3$  HDM catalyst designated RefNiMoP, containing 2 wt.% of NiO and 9 wt.% of  $MoO_3$  on a bimodal  $\gamma$  alumina, is also used for comparison with our model HPA-based catalysts. The solids in this study will be designated with letters: A, B and C according to the starting solutions used for their synthesis (V/Mo ratio: A = 1/11, B = 3/9 and C = 1) and will be associated to «Dry», «Cal» and «Sulph» according to the step of their preparation being considered, i.e. after drying, calcination and sulphidation respectively.

**Table 1**

Impregnating solution and oxidic precursor composition.

Impregnating solution				Oxidic precursor		
Designations	V/Mo atomic ratio	Molar ratio P/Mo	Molar ratio V/H <sub>2</sub> O <sub>2</sub>	Designations	MoO <sub>3</sub> (wt.%)	V <sub>2</sub> O <sub>5</sub> (wt.%)
A«Sol»	1/11	1/11	1/18	A«Cal»	9	0.54
B«Sol»	3/9	1/9	1/18	B«Cal»	9	1.91
C«Sol»	1	1/6	1/28	C«Cal»	9	5.74

## 2.2. Characterisation techniques

### 2.2.1. Raman spectroscopy

The species present in solution and on the oxidic precursors were characterised using Raman spectroscopy. The Raman spectra of the samples were recorded at room temperature using a Raman microprobe (Infinity from Jobin-Yvon), equipped with a photodiode array detector. The exciting laser source was the 532 nm line of an Nd-YAG laser. The wavenumber accuracy was 2 cm<sup>-1</sup>.

### 2.2.2. Nuclear magnetic resonance spectroscopy (NMR)

Nuclear magnetic resonance measurements were carried out on a spectrometer Avance 300 Bruker with broadband gradient z probes (BBO 10 mm and BBO 5 mm). The chemical shift was calibrated with a 1 M NaVO<sub>3</sub> solution for <sup>51</sup>V and 1 M phosphoric acid for <sup>31</sup>P. The spectra were recorded in liquid phase in the presence of a deuterium solvent.

### 2.2.3. Electron probe microanalysis (EPMA)

EPMA was performed on fresh catalyst with a JEOL 8800R microprobe to measure radial concentration profile of the metals in the catalyst spheres. For EPMA, 5 spheres were covered by a gold film and then embedded in a resin. The pieces of resin were then polished before recording the radial concentration profiles of Mo, V, Al and P and thus reporting the mean radial concentration profile of the 5 spheres.

### 2.2.4. X-ray photoelectron spectroscopy (XPS)

XPS spectra were recorded using a KRATOS AXIS Ultra spectrometer equipped with a (150 W) Al K $\alpha$  monochromatic source (1486.6 eV) and a hemi-spherical analyser operating at fixed pass energy of 40 eV. For sulphided catalysts, the sample preparation was carried out under controlled atmosphere (Ar with O<sub>2</sub> and H<sub>2</sub>O < 15 ppm) in order to avoid the partial reoxidation of the catalysts. The decomposition of the S 2p, Mo 3d and V 2p XPS spectra was performed using the appropriate reference sulphided samples (alumina-supported V<sub>x</sub>S<sub>y</sub> and MoS<sub>2</sub>) and the literature data. Binding energies are reported relative to C 1s contamination line at 284.6 eV. The curves were integrated applying a Shirley type baseline and Gaussian (30%)–Lorentzian (70%) decomposition parameters. The collected spectra were analysed using CasaXPS software, Version 2.0.71. For each catalyst, the metal and sulphur peaks have been identified according to their binding energies.

### 2.2.5. Transmission electron microscopy (TEM)

The transmission electron microscopy studies (TEM) were performed on a FEI Tecnai FEG microscope in order to determine the average length and stacking of the MoS<sub>2</sub> slabs by counting at least 350 particles. The sample was prepared following three different steps. The catalyst was first grinded and then dispersed in ethanol using an ultrasonic device. Two drops of the latter solution were deposited on a carbon-coated Cu grid and the solvent was evaporated under infrared light. The sample was introduced into the microscope and vacuum was made in the analysis room (8.2  $\times 10^{-7}$  Torr). Analysis was carried out on different areas of the sample.

## 2.3. Catalytic activity

### 2.3.1. Toluene hydrogenation and cyclohexane isomerisation catalytic test

Catalytic activity measurements in toluene hydrogenation (HYD) and cyclohexane isomerisation (ISOM) were carried out in a fixed-bed high pressure down-flow microreactor at 623 K under a total pressure of 6 MPa (PH<sub>2</sub> = 4 MPa) with 4 ml of catalyst diluted in 4 ml of carborundum (SiC). The liquid hourly space velocity (LHSV) was 1 h<sup>-1</sup> and the hydrogen to feed ratio was 450 NL/L (equal to the ratio between the volume of hydrogen and the volume of feed at a pressure of 1 atmosphere and at room temperature). The model feed was composed of dimethyldisulphide (DMDS, 5.9 wt.%) and toluene (20 wt.%) in cyclohexane (74.1 wt.%). DMDS which is decomposed to CH<sub>4</sub> and H<sub>2</sub>S maintains the sulphided state of catalysts during test.

Prior to catalytic tests, the same feedstock was used for the *in situ* presulphidation of the catalysts. The sulphidation was conducted at a total pressure of 6 MPa and at a temperature of 623 K with a ramp of 5 K/min from room temperature and at the same hydrogen to feed ratio conditions as for the catalytic test whereas LHSV was higher, 4 h<sup>-1</sup>.

The liquid products of the reactions were analysed by gas chromatography using a PONA column heated from 313 K to 393 K and a flame ionisation detector at 573 K. For these catalytic tests, the duration was 6 h long, the steady state being generally reached after 2 h on stream. First order kinetic laws were used to report the HYD and ISOM activities. Considering a plug flow reactor, volumic activity was obtained from the following expressions:

$$\text{HYD conversion (\%)} = \frac{\sum \text{Toluene products } x_i}{x_{\text{Toluene}} + \sum \text{Toluene products } x_i}$$

$$\text{Volumic activity (h}^{-1}\text{)} = \text{LHSV} \times \ln \left( \frac{1}{1 - \text{HYD conversion}} \right)$$

The activity per mole Mo + V can then be obtained with the following equation:

$$\begin{aligned} \text{Activity per mole of Mo + V (h}^{-1}\text{/mole Mo + V}^{-1}\text{)} \\ = \frac{\text{LHSV} \times \ln \left( \frac{1}{1 - \text{HYD conversion}} \right)}{\text{Density of catalyst} \times \text{Volume of catalyst} \times \left( \frac{\% \text{Mo}}{M_{\text{Mo}}} + \frac{\% \text{V}}{M_{\text{V}}} \right)} \end{aligned}$$

in which the term “Density of catalyst  $\times$  Volume of catalyst” corresponds to the mass of catalyst which can be charged for a given reactor volume and  $M_{\text{Mo}}$  and  $M_{\text{V}}$  correspond to the molecular weight of the Mo and V respectively.

### 2.3.2. Residue hydrotreatment catalytic test

Residue catalytic tests were carried out in a 300 mL batch reactor operated in fixed-bed conditions. The feed used was a Safaniya VR (vacuum residue), the characteristics of which are reported in Table 2.

The experimental conditions employed were a total pressure of 9.5 MPa, a reaction temperature at 643 K, a stirring rate of 800 rpm and a reaction time of 2 h. A catalyst volume of 15 mL was used to treat 90 mL of feed. The catalyst was presulphided *ex situ* during 2 h

**Table 2**  
Properties of Safaniya crude vacuum residue.

Ni (ppm)	45
V (ppm)	142
Ni + V (ppm)	187
S (wt.%)	4.8
C <sub>7</sub> -Asphaltenes (wt.%)	13.9
Conradson carbon residue (wt.%)	20.0
Density (SI units)	1.03

at atmospheric pressure and at a temperature of 623 K with a H<sub>2</sub>/H<sub>2</sub>S (15% mol.) mixture and a gas flow of 2 L/h/g<sub>catalyst</sub>. We here choose to evaluate the initial activities in order to evaluate the effect of the vanadium introduced in the preparation because V deposition occurs during the test and the value deduced would then correspond to the reactivity of the catalyst after vanadium deposition.

S and V contents of feed and effluents were measured by X-ray fluorescence. Asphaltene is defined as the fraction soluble in hot toluene and insoluble in *n*-heptane. From these data the various conversions (HDX) determined were hydrodesulphurisation (HDS), hydrodevanadisation (HDV) and hydrodeasphaltenisation (HDA<sub>SC7</sub>).

### 3. Results and discussion

#### 3.1. Characterisation of the impregnating solutions

The nature of species obtained in solution were characterised by Raman spectroscopy. Fig. 1 shows the Raman spectra of the solutions recorded at room temperature. They exhibit characteristic lines at 990 cm<sup>-1</sup> and 970 cm<sup>-1</sup> corresponding to Mo–O<sub>t</sub> (where *t* stands for terminal Mo–O bond) stretching vibrations whichever the V/Mo ratio. A large line at 607 cm<sup>-1</sup> is also observed and it is assigned to a Mo–O–Mo vibration whereas the line at 257 cm<sup>-1</sup> is assigned to a Mo–O–Mo bending mode. These Raman lines can be assigned by reference to the literature data [28] to Keggin substituted heteropolyanions PMo<sub>(12-x)</sub>V<sub>x</sub>O<sub>40</sub><sup>(3+x)-</sup>. UV–visible spectroscopy (not shown here) confirmed the presence of Mo<sup>6+</sup> and V<sup>5+</sup> species in solution [29,30]. Furthermore, characterisation of the RefMoP catalyst impregnating solution by Raman spectroscopy (spectra not reported here) shows the presence of the diphosphore pentamolybdenum HPA [27].

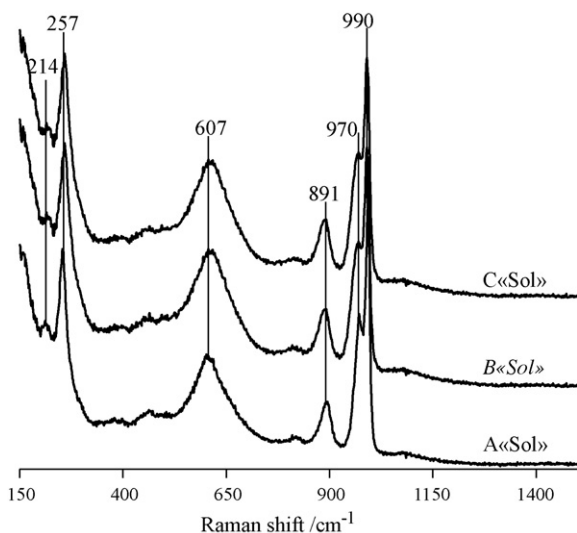


**Fig. 1.** Raman spectra of impregnating solutions PMo<sub>(12-x)</sub>V<sub>x</sub>O<sub>40</sub> for *x* = 1 (A«Sol»), *x* = 3 (B«Sol») and *x* = 6 (C«Sol»).

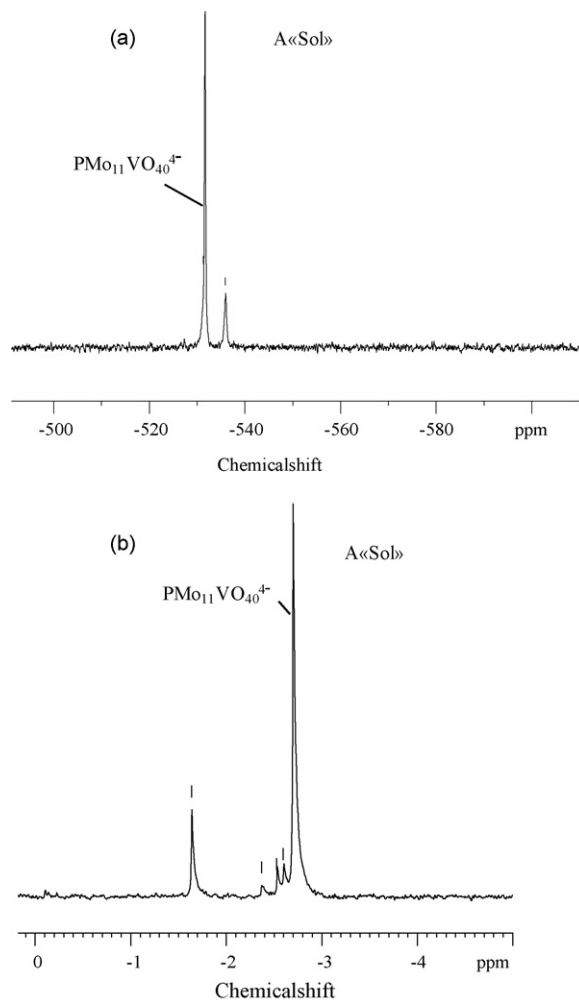


**Fig. 2.** <sup>51</sup>V (a) and <sup>31</sup>P NMR (b) spectra of PMo<sub>(12-x)</sub>V<sub>x</sub>O<sub>40</sub> solution with *x* = 1 (A«Sol»).

NMR spectroscopy was necessary to more clearly define the HPA. This analysis made it possible to discriminate the different heteropolyanions with reference to the literature knowledge. The <sup>51</sup>V and <sup>31</sup>P spectra obtained for A«Sol» are reported in Fig. 2(a) and (b). The <sup>51</sup>V spectrum exhibited a main line at -531.7 ppm and the <sup>31</sup>P spectrum showed an intense signal at -2.7 ppm. These chemical shifts correspond to the Keggin-type HPA PMo<sub>11</sub>VO<sub>40</sub> as suggested by Odyakov et al. [26] but they are lower than those observed by Pettersson et al. [31] (-533.6 on <sup>51</sup>V and at -3.7 ppm on <sup>31</sup>P). These authors demonstrated that the variation in chemical shift was due to the pH of the solution since the species came to be protonated as from pH ≈ 2. In our case, the pH of the solutions at 298 K was ≈ 2.2 so the chemical shifts are in agreement with Pettersson et al. [31]. Weaker signals in <sup>51</sup>V and <sup>31</sup>P spectra are attributed to a low quantity of PMo<sub>10</sub>V<sub>2</sub>O<sub>40</sub><sup>5-</sup> species as seen hereafter. The HPA PMo<sub>11</sub>VO<sub>40</sub> was used as an internal <sup>51</sup>V and <sup>31</sup>P chemical shift standard thereafter.

The NMR <sup>51</sup>V spectra for B«Sol» and C«Sol» are shown in Fig. 3(a) and (b). The NMR results are in agreement with the literature data [31] which demonstrated the presence of different heteropolyanions and their isomers when two or more molybdenum were substituted with vanadium. On the B«Sol» spectrum (Fig. 3(a)), we observed three groups of signals which are assigned to PMo<sub>11</sub>VO<sub>40</sub><sup>4-</sup> (-531.8 ppm), to PMo<sub>10</sub>V<sub>2</sub>O<sub>40</sub><sup>5-</sup> and its two isomers (-527.5, -535.1 and -537.6 ppm) and finally to PMo<sub>9</sub>V<sub>3</sub>O<sub>40</sub><sup>6-</sup> and its two isomers (from -540 to -545 ppm). The spectrum obtained for C«Sol» was large and presented signals which may be

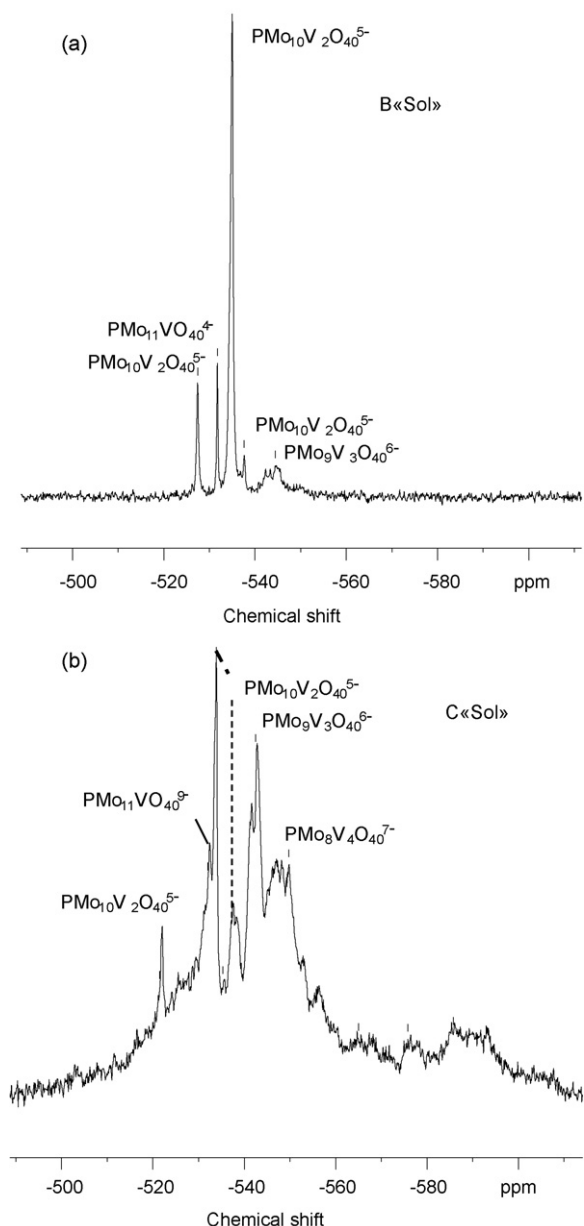


**Fig. 3.**  $^{51}\text{V}$  NMR spectra of  $\text{PMo}_{(12-x)}\text{V}_x\text{O}_{40}$  solution with  $x=3$  (B«Sol») (a) and with  $x=6$  (C«Sol») (b).

ascribed to different heteropolyanions and their isomers just as for B«Sol». The effect of pH on the chemical shifts suggested by Pettersson et al. [31] as mentioned earlier was also observed for these two solutions. In the same way the  $^{31}\text{P}$  NMR spectra (not shown here) confirmed the presence of different types of Keggin HPA  $\text{PMo}_{(12-x)}\text{V}_x\text{O}_{40}$  with their isomers in solution. Thus by increasing the vanadium loading,  $\text{PMo}_{10}\text{V}_2\text{O}_{40}^{5-}$  is the main HPA in the B«Sol» and the HPAs  $\text{PMo}_{10}\text{V}_2\text{O}_{40}^{5-}$ ,  $\text{PMo}_9\text{V}_3\text{O}_{40}^{6-}$  and  $\text{PMo}_8\text{V}_4\text{O}_{40}^{7-}$  are mainly identified in C«Sol», indicating that in solution different  $\text{PMo}_{(12-x)}\text{V}_x\text{O}_{40}^{(3+x)-}$  species are in equilibria.

### 3.2. Characterisation of the oxidic precursors

#### 3.2.1. The solids after the drying step

In order to verify the penetration of the HPA inside the extrudates, electron probe microanalysis (EPMA) of the dried solids was performed. We saw previously that increasing the vanadium content increased the number of different Keggin substitute HPAs in

equilibria. A heterogeneity of molybdenum and vanadium could be expected at high vanadium content. The distribution of metals in one of the beads analysed for both solids are presented on Fig. 4. Analysis revealed a homogeneous distribution of metals in the grains of these catalysts with an almost flat radial concentration for vanadium and molybdenum. In a general way, we can consider that the metals should also be well distributed in A«Dry».

Fig. 5 shows the Raman spectra for the three solids (A«Dry», B«Dry» and C«Dry») after drying. The spectrum for A«Dry» exhibits main lines around  $990\text{ cm}^{-1}$ ,  $969\text{ cm}^{-1}$  and  $615\text{ cm}^{-1}$  which are assigned to Keggin substituted heteropolyanions  $\text{PMo}_{(12-x)}\text{V}_x\text{O}_{40}$  [28]. However a partial decomposition may occur if we consider the variation in the relative intensity of these lines. For B«Dry» main lines are observed at  $959\text{ cm}^{-1}$  and  $969\text{ cm}^{-1}$  coupled with low frequency lines at  $715\text{ cm}^{-1}$ ,  $371\text{ cm}^{-1}$  and  $243\text{ cm}^{-1}$ . They can be ascribed by reference to the literature [28] to Keggin lacunary polyanions such as  $\text{PX}_{11}\text{O}_{39}$  or  $\text{PX}_9\text{O}_{34}$  where X can be either Mo or V. In our case the presence of  $\text{PMo}_{11}\text{O}_{39}$  or  $\text{PMo}_9\text{O}_{34}$  entities in the solid state could be explained by the formation of lacunary entities stabilised on the support which could not exist in solution. Finally a main line at  $888\text{ cm}^{-1}$  with a shoulder line at  $992\text{ cm}^{-1}$  is observed for the solid at high vanadium content (C«Dry»). These lines can be ascribed to polyvanadate species since these lines were also put into evidence by Payen and co-workers on a vanadium/ $\text{Al}_2\text{O}_3$ -supported solid after drying [32]. We can conclude that the monosubstituted Keggin HPA is more stable whereas at high vanadium loading  $\text{PMo}_{(12-x)}\text{V}_x\text{O}_{40}$  [28] and lacunary species are formed on alumina. The increase in vanadium content also leads to the observation of only vanadium species by Raman spectroscopy.

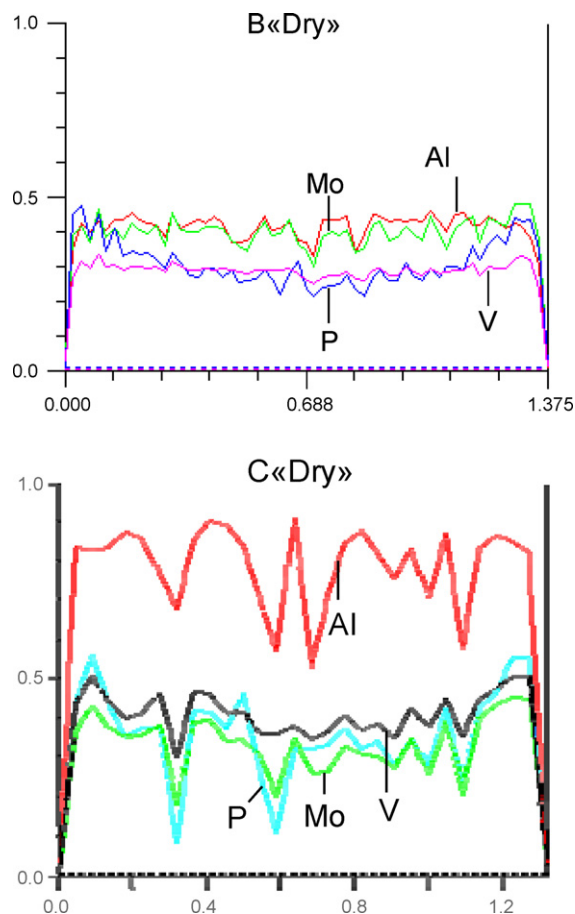


**Fig. 4.** EPMA radial concentration for  $\text{V}/\text{Mo}=3/9$  (B«Dry») and  $\text{V}/\text{Mo}=1$  (C«Dry») after drying.

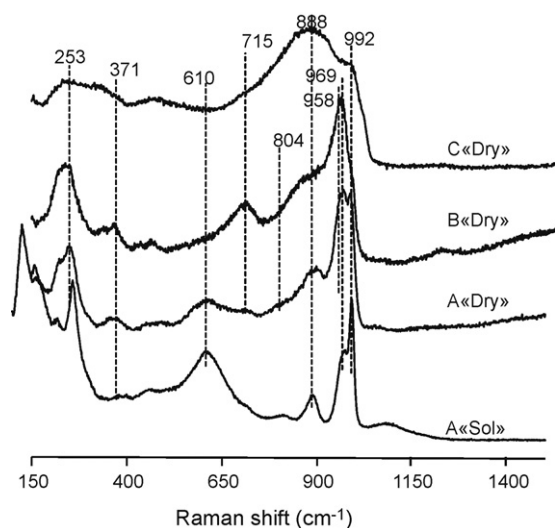


**Fig. 5.** Raman spectrum of impregnating solution for  $\text{PMo}_{(12-x)}\text{V}_x\text{O}_{40}$  for  $\text{V}/\text{Mo} = 1/11$  (A«Sol») and Raman spectra of solids after drying:  $\text{V}/\text{Mo} = 1/11$  (A«Dry»),  $\text{V}/\text{Mo} = 3/9$  (B«Dry») and  $\text{V}/\text{Mo} = 1$  (C«Dry»).

It should be mentioned that the Raman spectrum of the dried solid A«Dry» exhibits the main features of the impregnating solution (Fig. 1), which allows us to state at least on its partial preservation on the support. However, due to the presence of lacunary anions at higher vanadium content, we can thus conclude on the partial presence of Keggin substituted and lacunary anions on the solids after drying. A tentative suggestion for the formation of lacunary species may be due to a change in pH of the impregnating solution in the course of its diffusion in the porous network of the support because of the buffer effect of alumina at low molybdenum loading [33]. According to speciation diagrams [34], increase in pH indeed favours the formation of lacunary Keggin heteropolyanions  $\text{PX}_{11}\text{O}_{39}$  or  $\text{PX}_9\text{O}_{34}$  which become the major species for pH greater than 3.

### 3.2.2. Calcined solids

After calcination, we observe that the Raman spectra for the three solids, A«Cal», B«Cal» and C«Cal» (Fig. 6), did not exhibit the mainlines corresponding to the starting Keggin substituted HPA ( $990\text{ cm}^{-1}$  and  $970\text{ cm}^{-1}$ ). We can thus conclude that this HPA no longer exists after calcination. A main dissymmetrical line around

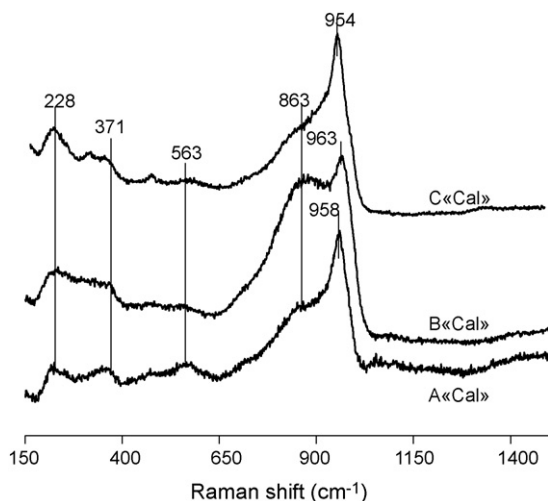


**Fig. 6.** Raman spectra after calcination at 773 K of the oxidic precursors:  $\text{V}/\text{Mo} = 1/11$  (A«Cal»),  $\text{V}/\text{Mo} = 3/9$  (B«Cal») and  $\text{V}/\text{Mo} = 1$  (C«Cal»).

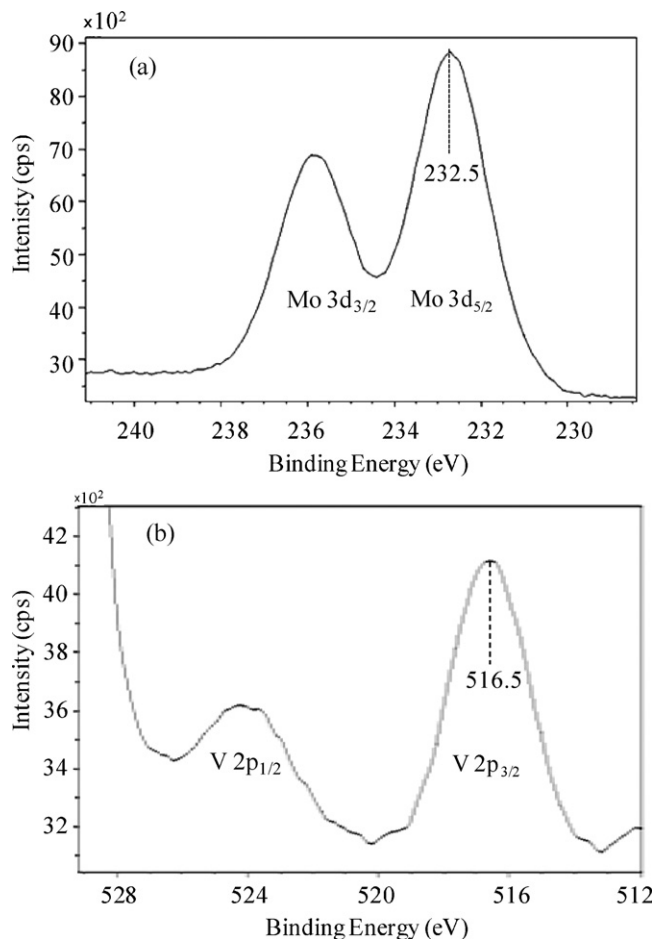


**Fig. 7.** XPS spectra of the oxidic precursor at  $\text{V}/\text{Mo} = 3/9$  (B«Cal») for Mo (a) and for V (b).

$960\text{ cm}^{-1}$  with a shoulder at  $863\text{ cm}^{-1}$  is observed for the three oxidic precursors. This line is tentatively assigned to the formation of a well dispersed polymolybdate [35] or polyvanadate phase [32]. Moreover Raman spectroscopy did not exhibit any crystalline species such as  $\text{V}_2\text{O}_5$  or  $\text{MoO}_3$ .

Further analyses were carried out after calcination on the B«Cal» and C«Cal» (not shown here) catalysts using XPS analysis. Fig. 7 shows the Mo 3d (a) and the V 2p (b) spectra for B«Cal». The photopeak of Mo 3d<sub>5/2</sub> on the oxidic precursor is positioned at 232.5 eV and can be ascribed to the  $\text{Mo}^{6+}$  in an oxide environment, thus surface polymolybdates in our case [36]. Moreover a broadening of the photopeak was observed ( $>2\text{ eV}$ ) indicating either the presence of multiple species with chemical characteristics not perfectly defined [37] or an interaction between the precursors Mo, V with either P or the support [38,39].

The spectrum of V 2p<sub>3/2</sub> spectra for B«Cal» is reported in Fig. 7 (b) and a main broad band with an apparent maximum at 516.5 eV is observed. Two possible species in an oxide environment [40] could be put into evidence:  $\text{V}^{5+}$  (BE  $\approx 517.2\text{ eV}$ ) and  $\text{V}^{4+}$  (BE  $\approx 516.1\text{ eV}$ ) in agreement with literature data. Muller et al. also showed that the binding energy of oxygenated vanadium lied between 516.2 eV and 517.4 eV [41] and Wang et al. suggested that those of the different vanadium valences go from 512 eV to 517 eV [42].

### 3.3. Characterisation of the sulphided catalysts

The XRD diffractogram (not shown here) did not evidence the formation of any crystalline phase other than aluminium oxide for the catalysts B«Sulph» and C«Sulph».

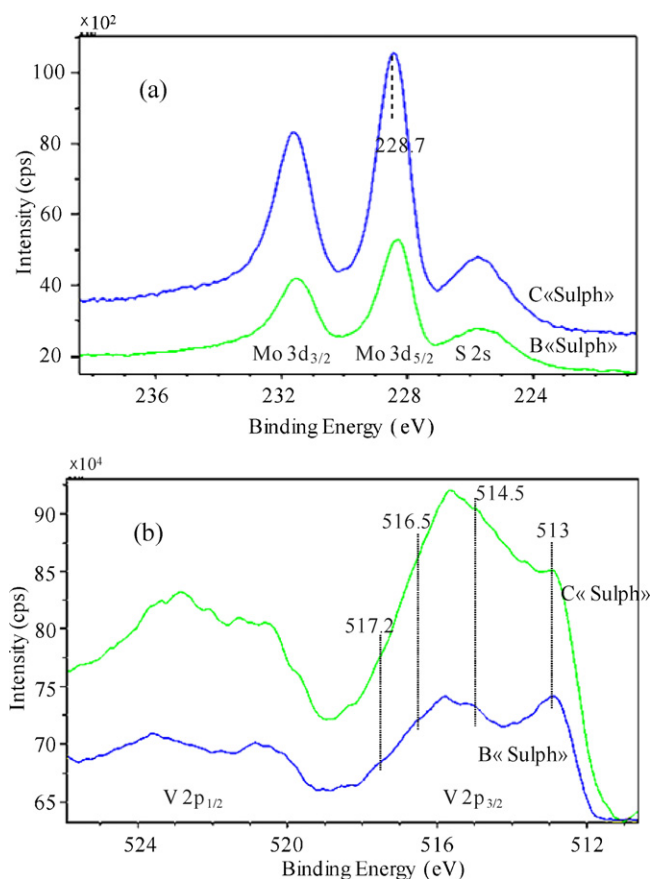


**Fig. 8.** XPS spectra of V/Mo = 3/9 (B«Sulph») and 1 (C«Sulph») after sulphidation at 623 K for Mo (a) and for V (b).

The dispersion and the nature of the active sulphided species for the catalysts B«Sulph» and C«Sulph» were then characterised by XPS. On Fig. 8(a), we can see that the binding energy for Mo 3d<sub>5/2</sub> has shifted to 228.7 eV after sulphidation. This binding energy is characteristic of Mo<sup>4+</sup> in a sulphur environment as in MoS<sub>2</sub> [43,44]. The signal around 225.5 eV corresponds to the S 2s contribution.

The V 2p spectra for the sulphided solids (B«Sulph» and C«Sulph») are presented in Fig. 8(b). The spectra exhibit large V 2p doublets. From decomposition, two vanadium species in a sulphur environment were mainly put into evidence: (V2p<sub>3/2</sub>)<sup>2+</sup> (BE ≈ 513 eV) and (V2p<sub>3/2</sub>)<sup>4+</sup> (BE ≈ 514.5 eV). However, since the signal is quite broad, oxidised species may also be present. The photopeaks at 517.4 eV and 516.5 eV may thus be assigned to V<sup>5+</sup> and V<sup>4+</sup> respectively in an oxide environment [41] (Fig. 7). This suggests the partial sulphidation of vanadium (~55%) in our sulphidation conditions as reported by Janssens et al. [45]. They showed that supported vanadium catalyst underwent partial sulphidation at low temperatures which led to the formation of both highly dispersed species and poorly dispersed vanadium species. Moreover, they put into evidence that bulk vanadium sulphidation is predominant at high temperatures with V<sub>2</sub>O<sub>5</sub> being quantitatively sulphided to V<sub>2</sub>S<sub>3</sub> at 1273 K.

In addition to XPS, transmission electron microscopy was used to assess the morphology of the sulphided phase for B«Sulph» (Fig. 9) and C«Sulph» (not presented here). Well dispersed MoS<sub>2</sub> crystallites having mean lengths between 3 nm and 4 nm were identified. The average stacking was between 1 and 2. Vanadium or molybdenum sulphide aggregates were not observed during analysis. Moreover energy dispersive X-ray (EDX) analysis always evidenced vanadium with MoS<sub>2</sub> slabs. Thus it seems that vanadium is well dispersed on the catalyst but we cannot conclude on its exact

location: as a promoter of the active phase or as a well dispersed phase on the alumina support.

### 3.4. Catalytic performances in model and real feedstock

#### 3.4.1. Toluene hydrogenation and cyclohexane isomerisation catalytic test

Hydrogenation (HYD) and isomerisation (ISOM) activities for the model HPA-based catalysts were measured on a model feed. Fig. 10 shows the volumic activities (activity per volume of catalyst) for hydrogenation of toluene (Fig. 10(a)) and for isomerisation of cyclohexane (Fig. 10(b)) as a function of the vanadium loading. The activities of a RefMoP/Al<sub>2</sub>O<sub>3</sub> catalyst are also reported in Fig. 10. The hydrogenation activity (HYD) of the model catalysts increases with the vanadium loading and is much higher than that of the reference catalyst. The same evolution is observed for isomerisation and this may be related to the acidity brought by vanadium which favours isomerisation reactions. A clear increase in HYD activity is observed for C«Cal» catalyst (V/Mo = 1) as compared to the reference catalyst. This improvement may be induced by either a V<sub>x</sub>S<sub>y</sub> phase or a V–Mo–S phase as was shown by Hubaut et al. [22]. Furthermore, this result is in agreement with the well dispersed active phase observed with TEM.

#### 3.4.2. Residue hydrotreatment catalytic test

Tests using a Safaniya feed were also undertaken on the model catalysts and the results were compared to reference catalysts Ref-MoP and RefNiMoP. The removal rates of sulphur, vanadium and asphaltenes are reported relatively to the RefMoP catalyst.

The effect of V on HDS activity is rather different than that of nickel as shown in Fig. 11. The sulphur removal rate are also reported in Fig. 11. When considering the errors related to the test we can assert that the vanadium-based catalysts do not seem to have much effect on HDS as compared to RefNiMoP. Guillard and co-workers [11] showed that unsupported vanadium catalysts had little effect on HDS activity. It can be concluded that vanadium has very little effect on the active phase as compared to nickel.

HDV (hydrodevanadation) and HDAsC<sub>7</sub> (HDasphaltenes) conversions are reported in Fig. 12(a) and (b) on which are also reported

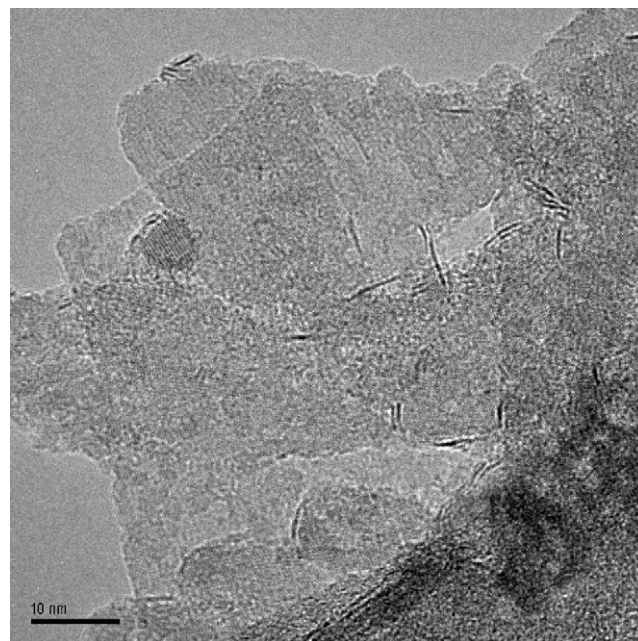


**Fig. 9.** TEM micrograph of the V/Mo = 3/9 (B«Sulph») catalyst.

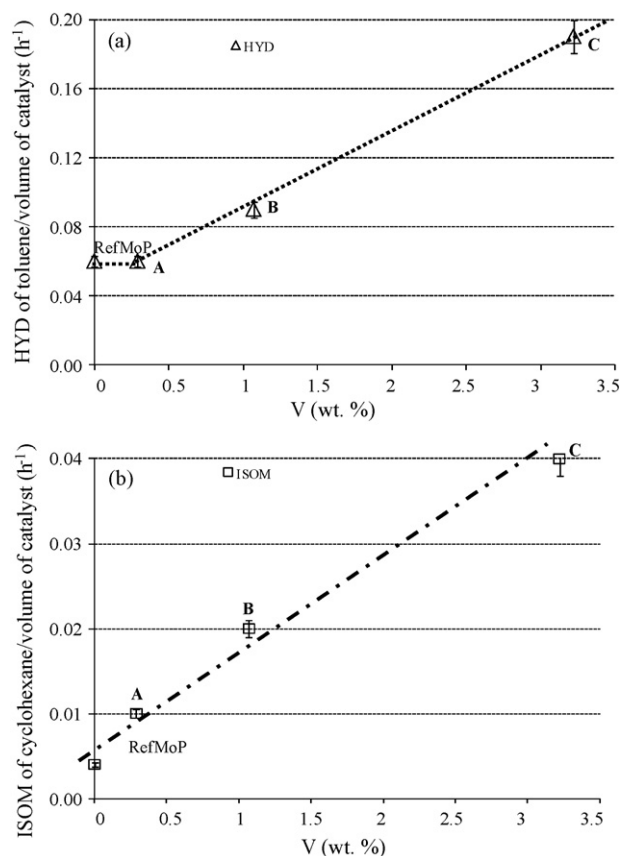


**Fig. 10.** Volumic activities of hydrogenation of toluene (a) and isomerisation of cyclohexane (b) with use of model catalysts and RefMoP catalyst (error bar estimated).

the relative conversions to RefMoP catalyst. Vanadium seems to have an influence on these conversions as compared to the RefMoP catalyst. A«Cal» catalyst (V/Mo = 1/11) seems the most effective showing approximately the same conversion for both HDV and HDAsC<sub>7</sub> as a RefNiMoP catalyst which is a standard catalyst for HDM and HDAsC<sub>7</sub>. A slight decrease is observed for B«Cal» and C«Cal» catalysts but the conversions are still higher than for RefMoP. These results may be linked to a well dispersed active phase or furthermore linked to the influence of vanadium.

It has been shown that HDAsC<sub>7</sub> is essential for hydrodemetallation reactions since large asphaltenic entities must unbound porphyrins for HDM reactions [46]. HDAsC<sub>7</sub> and HDM may thus be enhanced by either a V-sulphide phase or V–Mo–S phase. Dejonghe et al. [23] showed that, in the presence of vanadium from the feed, nickel in the Ni–Mo–S phase was gradually replaced to give way to a VMoS phase which was much less active than the Ni–Mo–S phase.

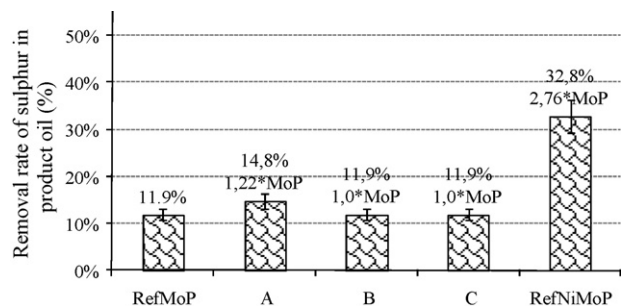


**Fig. 11.** HDS: removal rate of sulphur in product oil (error bar estimated) and relative removal of sulphur to RefMoP catalyst.

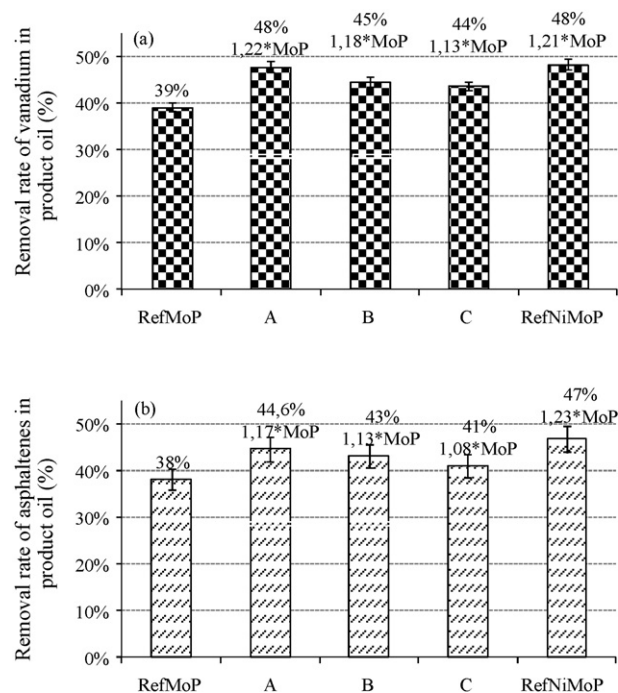


**Fig. 12.** Vanadium removal rate (a) and AsC<sub>7</sub> removal rate (b) from product oil (error bar estimated). The relative removal of vanadium and asphaltenes to RefMoP catalyst is also indicated.

The vanadium incorporated in VMoS may be more active for HDM and HDAsC<sub>7</sub> than vanadium sulphides as was showed by Takeuchi et al. [17] during the hydrotreatment of heavy oil with bare alumina. Sasaki et al. [47] reported a comparative study made on NiV/Al<sub>2</sub>O<sub>3</sub> and CoMo/Al<sub>2</sub>O<sub>3</sub> which showed that the NiV catalyst could have an activity comparable to a CoMo for the demetallation of residues. The use of Ni–V sulphides was also suggested by Betancourt et al. [48] more recently. Therefore, it seems highly likely that a new active site formed from V and Mo could be responsible for the high activity of the model catalysts in HDM and HDAsC<sub>7</sub>.

### 3.5. Discussion

HDM catalysts have been prepared from solutions containing Keggin substituted heteropolyanions in which molybdenum and vanadium were introduced in the same structure. The solution was impregnated on an alumina support by the incipient wetness method. The evolution of the HPA was followed by different characterisations at the different steps of the preparation of the oxidic precursor. A mixture of different Keggin substituted HPAs and their isomers were observed in the impregnating solutions at high vanadium loading. After impregnation, the Keggin substituted HPA was mainly preserved at low vanadium loading only. It seems that the Keggin monosubstituted HPA is more stable than the other substituted heteropolyanions. Keggin lacunar species were also observed to mainly form on B«Dry». The formation of these species may be explained by the instability of  $\text{PMo}_{12-x}\text{V}_x^{(3+x)-}$  species other than  $\text{PMo}_{11}\text{VO}_{40}^{4-}$ . Lacunary species could form through interaction with the support. At high vanadium loading, well dispersed polyvanadate species were identified by Raman spectroscopy on C«Dry». After calcination, the formation of polyvanadate and polymolybdate species were evidenced showing the high dispersion of both metals on the alumina support. In the sulphidated state, well dispersed MoS<sub>2</sub> nanocrystallites were evidenced but their size does not seem to be modified by the use of these new oxidic precursors. XPS analysis indicated that vanadium could be in either a VS or a

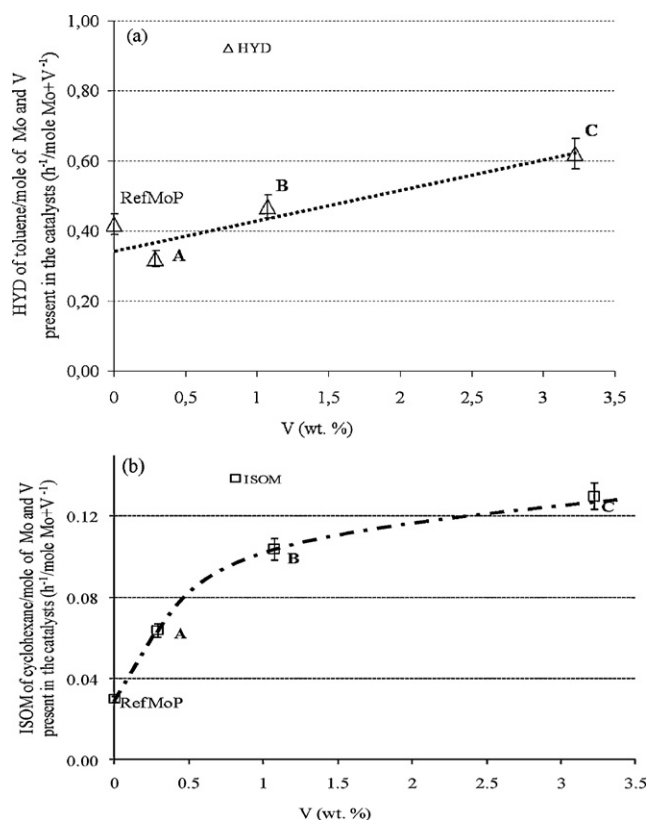


**Fig. 13.** Activities of hydrogenation of toluene (a) and isomerisation of cyclohexane (b) per mole of Mo and V present in the catalysts (error bar estimated).

$\text{VS}_2$  form but we could not conclude on the exact location of the vanadium although it was always identified with  $\text{MoS}_2$  slabs.

Hydrogenation of toluene and isomerisation of cyclohexane tests show that the use of vanadium in molybdenum catalysts brings on a synergy effect which increases with the vanadium loading as compared to a RefMoP catalyst. This synergy effect can be observed in Fig. 13 which reports the activity of hydrogenation of toluene and isomerisation of cyclohexane per mole of metals (molybdenum + vanadium) present in the catalysts. It clearly shows the improvement with the V content. This beneficial effect was also observed on HDM and HDAsC<sub>7</sub> that could in part be related to the improvement of hydrogenation and/or isomerisation, the latter being improved by the presence of vanadium.

The use of Keggin substituted HPA in which Mo and V are in the same structure as starting material seems to be favourable for the preparation of new HDM catalysts as their activity is higher than the RefMoP one that is prepared with a heteropolymolybdate solution. An optimum V/Mo ratio for HDM and HDAsC<sub>7</sub> was observed with A«Cal» catalyst (V/Mo = 1/11). The preservation of Keggin monosubstituted HPA  $\text{PMo}_{11}\text{VO}_{40}^{4-}$  on the alumina support after drying can explain this effect. This promoting effect may thus be attributed to the direct interaction between molybdenum and vanadium which are inserted in the same HPA structure in the starting material and partially preserved upon deposition. This would inhibit the loss of vanadium atoms inside the alumina support after impregnation and thus lead to a good interaction between the V and the disulphide entities.

#### 4. Conclusion

New  $\text{MoV}/\text{Al}_2\text{O}_3$  oxidic precursors have been prepared with mixed heteropolyanions as starting material. It has been shown that these model catalysts exhibit catalytic improvement in the hydro-

genation of toluene and isomerisation of cyclohexane as compared to a conventional Mo reference catalyst. This is assigned to the good dispersion of both metals whatever the metal loading used in this work. An interesting HDM activity through HDV and a substantially higher HDAsC<sub>7</sub> activity similar to a RefNiMoP catalyst which is generally used for heavy oil hydrotreatment are also observed for the low V content.

Heteropolyanions containing molybdenum and vanadium appear as interesting new starting materials for the preparation of heavy oil hydrotreatment catalysts with improved performances.

#### Acknowledgements

The authors would like to acknowledge Georges Fernandes from the Catalysis by Sulphides Department and the Physics and Analysis Division for their collaboration in this work.

#### References

- [1] O.C. Mullins, H. Groenzin, *Energy Fuels* 14 (2000) 677.
- [2] O.P. Strausz, T.W. Mojelsky, E.M. Lown, I. Kowalewski, F. Behar, *Energy Fuels* 13 (1999) 228.
- [3] J.F. Lepage, S.G. Chatila, M. Davidson, In: IFP, Technip (Eds.) *Residue and Heavy Oil Processing Paris* (1992).
- [4] B.H. Cooper, B.B.L. Donnis, B. Moyse, *Oil Gas J.* 84 (1986) 39.
- [5] S. Kressman, D. Guillaume, M. Roy-Auberger, C. Plain, 14th Annual Saudi-Japanese Symposium: Catalysts in Petroleum Refining and Petrochemicals, Annual Catalysts in Petroleum Refining and Petrochemicals Symposium Papers, Dhahran, SAU, King Fahd University of Petroleum and Minerals, Research Institute, 2004, p. 38.
- [6] N.Y. Topsoe, H. Topsoe, *J. Catal.* 75 (1982) 354.
- [7] H. Topsoe, B.S. Clausen, E. Pedersen, *Ind. Eng. Chem. Fundam.* 25 (1986) 25.
- [8] H. Topsoe, B.S. Clausen, F.E. Massoth, in: J. Anderson, M. Boudart (Eds.), *Catalysis, Science and Technology*, vol. 11, Springer-Verlag, Berlin, 1996, p. 1.
- [9] A. Hauser, A. Marafi, A. Almutairi, A. Stanislaus, *Energy Fuels* 22 (2008) 2925.
- [10] R.A. Ware, J. Wei, *Am. Chem. Soc., Div. Petrol. Chem.* 30 (1985) 62.
- [11] M. Loos, I. Ascone, C. Goulon-Ginet, J. Goulon, C. Guillard, M. Lacroix, M. Breyse, D. Faure, T. Des Courieres, *Catal. Today* 7 (1990) 515.
- [12] J.B. Smith, J. Wei, *J. Catal.* 132 (1991) 1.
- [13] B.G. Silbernagel, *J. Catal.* 56 (1979) 315.
- [14] L.A. Rankel, *Am. Chem. Soc., Div. Petrol. Chem.* 26 (1981) 689.
- [15] L.A. Rankel, L.D. Rollman, *Fuel* 62 (1983) 44.
- [16] T.H. Fleisch, B.L. Meyers, J.B. Hall, G.L. Otis, *J. Catal.* 86 (1984) 147.
- [17] C. Takeuchi, S. Asaoka, S. Nakata, Y. Shiroto, *Prepr. - Am. Chem. Soc., Div. Petrol. Chem.* 30 (1985) 96.
- [18] B. Mocaer, J. Grimblot, T. Des Courieres, J. Bousquet, J.-P. Bonnelle, *Actes du Colloque Franco-Vénézuélien, IFP, Rueil Malmaison* (1985).
- [19] M.A. Callejas, M.T. Martinez, J.L.G. Fierro, C. Rial, J.M. Jiménez Mateos, F.J. Gómez-García, *Appl. Catal. A: Gen.* 220 (2001) 93.
- [20] S.T. Sie, *Stud. Surf. Sci. Catal.* 6 (1980) 545.
- [21] H. Toulhoat, J.C. Plumail, G. Martino, Y. Jacquin, *Prepr. - Am. Chem. Soc., Div. Petrol. Chem.* 30 (1985) 85.
- [22] R. Hubaut, C.F. Aissi, S. Dejonghe, J. Grimblot, *J. Chim. Phys.* 88 (1991) 1741.
- [23] S. Dejonghe, R. Hubaut, J. Grimblot, J.-P. Bonnelle, T. Des Courieres, D. Faure, *Catal. Today* 7 (1990) 569.
- [24] M.J. Ledoux, O. Michaux, S. Hantz, P. Panissod, P. Petit, J.J. Andre, H.J. Callot, *J. Catal.* 106 (1987) 525.
- [25] S. Yamamatsu, T. Yamaguchi, *Eur. Patent* 425 666 (1989), assigned to Asahi Chem. Co.
- [26] V.F. Odyakov, E.G. Zhizhina, R.I. Maksimovskaya, K.I. Matveev, *Kinet. Katal.* 36 (1995) 795.
- [27] P. Blanchard, C. Lamonier, A. Griboval, E. Payen, *Appl. Catal. A: Gen.* 322 (2007) 33.
- [28] G. Mestl, T. Ilkenhans, D. Spielbauer, M. Dieterle, O. Timpe, J. Kröhnert, F. Jentoft, H. Knözinger, R. Schlögl, *Appl. Catal. A: Gen.* 210 (2001) 13.
- [29] M.D. Argyle, K. Chen, C. Resini, C. Krebs, A.T. Bell, E. Iglesias, *J. Phys. Chem. B* 108 (2004) 2345.
- [30] S. Knobl, G.A. Zenkovets, G.N. Kryukova, R.I. Maksimovskaya, T.V. Larina, N.T. Vasinin, V.F. Anufrienko, D. Niemeyer, R. Schlögl, *Phys. Chem. Chem. Phys.* 5 (2003) 534.
- [31] L. Pettersson, I. Andersson, A. Selling, J.H. Grate, *Inorg. Chem.* 33 (1994) 982.
- [32] L.R. Le Coustumer, B. Taouk, M. Le Meur, E. Payen, M. Guelton, J. Grimblot, *J. Phys. Chem.* 92 (1988) 1230.
- [33] L. le Bihan, P. Blanchard, M. Fournier, J. Grimblot, E. Payen, *J. Chem. Soc. Faraday Trans.* 94 (1998) 937.
- [34] M. Arab, D. Bougeard, J.M. Aubry, J. Marko, J.F. Paul, E. Payen, *J. Raman Spectrosc.* 33 (2002) 390.
- [35] S. Kasztelan, J. Grimblot, J.P. Bonnelle, E. Payen, H. Toulhoat, Y. Jacquin, *Appl. Catal.* 7 (1983) 91.

- [36] T.A. Patterson, J.C. Carver, D.E. Leyden, D.M. Hercules, J. Phys. Chem. 80 (1976) 1700.
- [37] P. Ratnasamy, J. Catal. 40 (1975) 137.
- [38] N.K. Nag, J. Phys. Chem. 91 (1987) 2324.
- [39] T. Edmons, P.H. Mitchell, J. Catal. 64 (1980) 491.
- [40] M.A. Eberhardt, A. Proctor, M. Houalla, D.M. Hercules, J. Catal. 160 (1996) 27.
- [41] J.F. Muller, J.M. Magar, D. Cagniant, J.M. Mouchot, J. Grimblot, J.-P. Bonnelle, J. Organomet. Chem. 205 (1981) 329.
- [42] C.-M. Wang, T.-C. Tsai, I. Wang, J. Catal. 262 (2009) 206.
- [43] L. Benoist, D. Gonbeau, G. Pfister-Guillouzo, E. Schmidt, G. Meunier, A. Lev-asseur, Thin Solid Films 258 (1995) 110.
- [44] A.D. Gandubert, E. Krebs, C. Legens, D. Costa, D. Guillaume, P. Raybaud, Catal. Today 130 (2008) 149.
- [45] J.-P. Janssens, A.D. van Langeveld, J.A. Moulijn, Appl. Catal. A: Gen. 179 (1999) 229.
- [46] E. Furimsky, Catalyst for upgrading heavy petroleum feeds, Stud. Surf. Sci. Catal. 169 (2007) 1.
- [47] Y. Sasaki, Y. Ojima, T. Kondo, K. Ukegawa, A. Matsumura, T. Sakabe, J. Jpn. Petrol. Inst. 25 (1982) 27.
- [48] P. Betancourt, A. Rives, C.E. Scott, R. Hubaut, Catal. Today 57 (2000) 201.